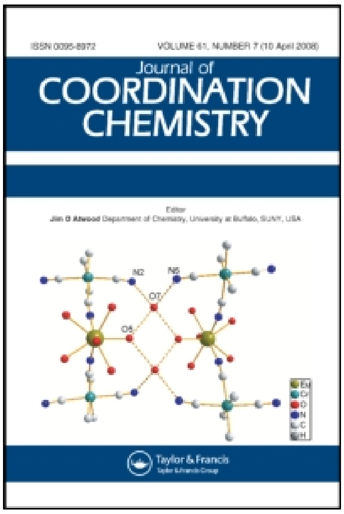

Journal of Coordination Chemistry
Publication details, including instructions for authors and subscription information:
http://www.informaworld.com/smpp/title~content=t713455674

Spectroscopic and thermal studies of [Fe(dioximato)$_2$(amine)$_2$] mixed chelates

Cs. Várhelyi Jr[a]; A. Kovács[b]; D. Nemcsok[c]; Z. Németh[d]; E. Kuzmann[e]; A. Vértes[d]; K. Vékey[f]; Cs. Várhelyi[g]; Gy. Pokol[c]
[a] Faculty of Chemistry, Babeş-Bolyai University, 400028-Cluj-Napoca Arany J. s. 11, Romania [b] Hungarian Academy of Sciences, Budapest University of Technology and Economics, H-1111 Budapest, Szt. Gellért tér 4 [c] Institute of General and Analytical Chemistry, H-1111 Budapest, Szt. Gellért tér 4, Hungary [d] Department of Nuclear Chemistry, Eötvös University, H-1117 Budapest, Pázmány P. sétány 1a, Hungary [e] Hungarian Academy of Sciences, Eötvös University, H-1117 Budapest, Pázmány P. sétány 1a, Hungary [f] Hungarian Academy of Sciences, Chemical Research Center, H-1525 Budapest, Hungary [g] Transylvanian Museum Association, 400009-Cluj-Napoca, Napoca s. 2, Romania

To cite this Article Várhelyi Jr, Cs. , Kovács, A. , Nemcsok, D. , Németh, Z. , Kuzmann, E. , Vértes, A. , Vékey, K. , Várhelyi, Cs. and Pokol, Gy.(2007) 'Spectroscopic and thermal studies of [Fe(dioximato)$_2$(amine)$_2$] mixed chelates', Journal of Coordination Chemistry, 60: 4, 379 — 392

To link to this Article: DOI: 10.1080/00958970600783969

URL: http://dx.doi.org/10.1080/00958970600783969

Journal of Coordination Chemistry
Vol. 60, No. 4, 20 February 2007, 379–392

Spectroscopic and thermal studies of $[Fe(dioximato)_2(amine)_2]$ mixed chelates

Cs. VÁRHELYI Jr*†, A. KOVÁCS‡, D. NEMCSOK§, Z. NÉMETH¶,
E. KUZMANN‖, A. VÉRTES¶, K. VÉKEY⊥, Cs. VÁRHELYI° and
Gy. POKOL§

†Faculty of Chemistry, Babeş-Bolyai University, 400028-Cluj-Napoca
Arany J. s. 11, Romania
‡Hungarian Academy of Sciences, Budapest University of Technology and Economics,
Research Group for Technical Analytical Chemistry, H-1111 Budapest, Szt. Gellért tér 4
§Institute of General and Analytical Chemistry, Budapest University of Technology and
Economics, H-1111 Budapest, Szt. Gellért tér 4, Hungary
¶Department of Nuclear Chemistry, Eötvös University, H-1117 Budapest,
Pázmány P. sétány 1a, Hungary
‖Hungarian Academy of Sciences, Eötvös University, Research Group for Nuclear Methods
in Structural Chemistry, H-1117 Budapest, Pázmány P. sétány 1a, Hungary
⊥Hungarian Academy of Sciences, Chemical Research Center, H-1525 Budapest,
Pf. 17, Hungary
°Transylvanian Museum Association, 400009-Cluj-Napoca, Napoca s. 2, Romania

(*Received 2 September 2005; in final form 29 November 2005*)

A number of mixed complexes of the type $[Fe(DioxH)_2(amine)_2]$ ($DioxH_2$ = glyoxime, dimethylglyoxime, methylethylglyoxime and benzylmethylglyoxime; amine = imidazole, benzimidazole, 2-methylimidazole, β- and γ-picoline, pyridine, *p*-toluidine, *p*-Cl-aniline, α-naphthylamine) have been prepared and characterised by FTIR, Mössbauer and mass spectroscopy. The structural and vibrational characteristics of the title complexes were modelled by quantum chemical (DFT) computations on $[Fe(methylglyoximato)_2(pyridine)_2]$. All the methods support strong Fe–N donor acceptor interactions and O–H $\cdots$ O hydrogen bonding in the complexes. The thermal behaviour of these non-electrolytic compounds was studied by TG, DTA and DTG measurements indicating a decomposition mechanism of $[Fe(DioxH)_2(amine)_2] \rightarrow [Fe(DioxH)_2(amine)] \rightarrow [Fe(DioxH)_2] \rightarrow [Fe(DioxH)] \rightarrow$ alkyl-, aryl-nitriles and hydrocarbon decomposition products.

Keywords: Iron-dioxime-amine complexes; FTIR spectroscopy, Mössbauer spectroscopy; Mass spectroscopy thermal analysis; DFT computations

1. Introduction

The formation of iron complexes with α-dioximes was reported first by Chugaev [1]. In contrast to the $[M(DioxH)_2]$ complexes with M = Ni, Pd, Pt which are insoluble in

---

*Corresponding author. Email: vcaba@chem.ubbcluj.ro

Journal of Coordination Chemistry
ISSN 0095-8972 print/ISSN 1029-0389 online
DOI: 10.1080/00958970600783969

water and soluble in some polar organic solvents, Fe(II) complexes are readily soluble in water. Crystallization is very difficult and, if obtained, crystals lack a well-defined composition (e.g. with $DH_2:2\ NaFe(DH)_2(OH) + 0.5–1.0\ Fe(DH)_2$ was obtained [2, 3]). In aqueous media, Fe(II)-dioximato complexes are very weakly rose coloured. The colour becomes darker and more intense in the presence of NH_3 or amines, indicative of formation of $[Fe(II)(DioxH)_2(amine)_2]$ type complexes. Feigl [4] obtained slightly soluble crystalline mixed complexes with aromatic or heterocyclic N-bases and tertiary phosphines. The latter complexes are suited for qualitative micro-analytical determination of iron.

Besides the popular dimethylglyoxime, a series of aromatic-, alicyclic- and heterocyclic α-dioximes were tested for analytical purposes [4–6]. The sensitivity of these reactions for iron are found to be influenced by the nature of the R*, R** substituents on the glyoxime skeleton. Note, however, that the selectivity and sensitivity of these methods do not reach those of the popular ones utilising $[Fe(\alpha,\alpha'\text{-dipyridile})_2]^{2+}$ and $[Fe(o\text{-phenanthroline})_2]^{2+}$ complexes.

In this article a series of mixed chelates of general formula $[Fe(DioxH)_2(amine)_2]$ with symmetric and asymmetric α-dioximes ($DioxH_2$ = glyoxime ($GlioxH_2$), dimethylglyoxime (DH_2), methylethylglyoxime ($Me\text{-}Et\text{-}GlyoxH_2$) and benzylmethylglyoxime ($Benz\text{-}Me\text{-}GlyoxH_2$) and various aromatic and N-heterocyclic amines (imidazole, benzimidazole, 2-methylimidazole, β- and γ-picoline, pyridine, *p*-toluidine, *p*-Cl-aniline, α-naphthylamine) are described. These complexes can be easily obtained by reaction of the components dissolved in alcohol at room temperature in inert atmosphere. We characterised the synthesised complexes by FTIR, Mössbauer and mass spectroscopy. The thermal decomposition was followed by thermal analysis (TG, DTG, DSC). To gain some general information on the structural and vibrational properties of such complexes, we performed quantum chemical computations on the $[Fe(methylglyoximato)_2(pyridine)_2]$ complex. Selection of the methylglyoxime ($Me\text{-}GlyoxH_2$) ligand facilitated an assessment of the relative stabilities of the structural isomers for asymmetric ($R^* \neq R^{**}$) $DioxH_2$ ligands.

Previous studies on $[Fe(DioxH)_2(amine)_2]$ compounds include magnetic and electron spectroscopic [7–12], thermoanalytical [13–15] and X-ray measurements [16–18] of some complexes. From the present series of complexes the IR spectrum and thermal decomposition of $[Fe(GlyoxH)_2(\gamma\text{-picoline})_2)]$ has been reported [15], and the structure of $[Fe(DH)_2(imidazole)_2]$ has been elucidated by X-ray diffraction [16]. The structures of transition metal dioxime complexes are summarised in the review of Chakravorty [19].

2. Experimental

2.1. *Syntheses*

2.1.1. Glyoxime. Fifty millilitre of 30% aqueous glyoxale was treated with an excess of hydroxylamine hydrochloride in conc. aqueous solution at room temperature. After 24 h, the formed white crystalline product was filtered and washed with ice-cooled water and dried in air.

2.1.2. Methylethylglyoxime and benzylmethylglyoxime. 0.1 mol of methyl-*n*-propylketone and 0.1 mol of benzylacetone in 100–100 mL ethanol were isonitroised at 0–5°C with gaseous ethylnitrite for 3–4 h. The yellow oil solutions (α-ketooximes) were treated with an excess of aqueous $NH_2OH \cdot HCl$ solution neutralised with NaOH. The mixtures were warmed on a water bath for 3–4 h, until the disappearance of the heterogeneous oily phase. After cooling to 0°C, the formed white crystalline products were filtered and recrystallised from ethanol. Yields: 40–70%.

2.2.3. [Fe(DioxH)$_2$(amine)$_2$] complexes. 0.01 mol of $[Fe(NH_4)_2(SO_4)_2] \cdot 6\,H_2O$ in 60–80 mL water and 0.02 mol of α-dioxime in 100 mL methanol or ethanol were mixed. After removal of the air from the solution by bubbling an inert gas (nitrogen or methane) for 10–15 min, 0.025 mol of amine in 20–25 mL alcohol was added and the bubbling of the inert gas was continued for another 10–15 min. The separated crystalline products were filtered off, washed with diluted methanol and dried in air. The reaction products were checked by complexometric titrations for Fe(II) and gas volumetric analysis for N. The difference between the calculated (expected) and found element content was ±0.1–0.35% for Fe and ±0.1–0.25% for N. Note that in some samples minor impurities belonging to unidentified complexes of Fe(II) and Fe(III) (including probably also solvent ligands) were indicated by Mössbauer measurements. These minor impurities, however, do not influence the main physico-chemical features reported in this paper. Some general characteristics of the title complexes are summarised in table 1.

Table 1. General characteristics of the [Fe(DioxH)(amin)$_2$] complexes.

No.	Formula[a]	Mol. wt. Calcd.	Yield (%)	Aspect
1	[Fe(GlioxH)$_2$(imidazole)$_2$]	366.1	55	Dark brown short irreg. plates
2	[Fe(GlioxH)$_2$(β-picoline)$_2$]	416.2	60	Brown dendrites
3	[Fe(GlioxH)$_2$(γ-picoline)$_2$]	416.2	70	Brown prisms
4	[Fe(GlioxH)$_2$(pyridine)$_2$]	388.2	50	Brown prisms
5	[Fe(Me-Et-GlyoxH)$_2$(pyridine)$_2$]	472.3	70	Brown rhomb. prism
6	[Fe(Me-Et-GlyoxH)$_2$(γ-picoline)$_2$]	500.4	75	Brown crops
7	[Fe(Me-Et-GlyoxH)$_2$(imidazole)$_2$]	450.3	60	Reddish brown microcryst.
8	[Fe(Benz-Me-GlyoxH)$_2$(pyridine)$_2$]	596.5	85	Brown crops
9	[Fe(Benz-Me-GlyoxH)$_2$(γ-picoline)$_2$]	624.5	90	Irreg. brown short plates
10	[Fe(Benz-Me-GlyoxH)$_2$(imidazole)$_2$]	574.4	80	Brown crops
11	[Fe(Benz-Me-GlyoxH)$_2$(benzimidazole)$_2$]	674.5	90	Short brown rhomb. prisms
12	[Fe(Benz-Me-GlyoxH)$_2$(*p*-toluidine)$_2$]	652.6	70	Brown dendrites
13	[Fe(Benz-Me-GlyoxH)$_2$(*p*-Cl-aniline)$_2$]	693.4	75	Brown crops
14	[Fe(Benz-Me-GlyoxH)$_2$(α-naphthylamine)$_2$]	724.6	90	Reddish brown dendrites
15	[Fe(DH)$_2$(pyridine)$_2$]	444.3	45	Reddish brown regulated prisms
16	[Fe(DH)$_2$(imidazole)$_2$]	422.2	75	Reddish brown crops
17	[Fe(OctoxH)$_2$(γ-picoline)$_2$]	580.5	75	Reddish brown crops
18	[Fe(OctoxH)$_2$(imidazole)$_2$]	530.4	85	Reddish brown short nidles
19	[Fe(Me-Et-GlyoxH)$_2$(benzimidazole)$_2$]	550.4	60	Reddish brown microcryst.
20	[Fe(Benz-Me-GlyoxH)$_2$(2-Me-imidazole)$_2$]	602.5	55	Brown plates
21	[Fe(Benz-Me-GlyoxH)$_2$(NH$_3$)$_2$]	472.3	43	Small brown plates

[a] Abbreviations of the α-dioximes: GlioxH$_2$ = glyoxime, Me-Et-GlyoxH$_2$ = methylethylglyoxime, DH = dimethylglyoxime, Benz-Me-GlyoxH$_2$ = benzylmethylglyoxime, OctoxH = cyclooctanedionedioxime.

2.2. *Spectroscopic and thermal measurements*

The FTIR spectra of the complexes were obtained from KBr and polyethylene pellets in the mid-IR (4000–450 cm^{-1}) and far-IR (650–150 cm^{-1}) range, respectively. The measurements were performed at room temperature on a Perkin Elmer System 2000 FTIR spectrometer operating with MCT detector in the mid-IR (16 scans) and DTGS detector in the far-IR (64 scans) range. The resolution was 4 cm^{-1}.

The mass spectrometric (MS) measurements were carried out by a VG ZAB2-SEQ tandem mass spectrometer in electron impact ionisation (EI) mode (ionisation energy: 70 eV, temperature of the ionic source: 200°C) and a PE Sciex API 2000 triple quadruple mass spectrometer using electrospray ionisation (ESI).

The ^{57}Fe Mössbauer spectra were recorded on powdered samples in the common transmission geometry. The applied γ-ray source was ^{57}Co(Rh) with 10^9 Bq activity. All spectra were taken at room temperature. Isomer shifts are given relative to α-iron.

The thermal measurements were performed with a 951 TG and 910 DSC calorimeter (DuPont Instruments) in Ar or N_2 atmosphere at a heating rate of 10 K min^{-1} (sample mass 4–10 mg).

2.3. *Computations*

The quantum chemical calculations on two isomers of [Fe(Me-GlyoxH)$_2$(pyridine)$_2$] were carried out with the GAUSSIAN 98 program package [20] using the Becke3-Lee-Yang-Parr (B3-LYP) exchange-correlation functional [21, 22]. The relativistic effective core potential and its [341/311/41] valence basis set of Hay and Wadt [23] were used for Fe. The 6-31G** basis set was applied for H, C, O, and N. The minimum character of the optimised structures was verified by frequency calculations. The relative stability of the two isomers was evaluated from the computed absolute energies after zero-point vibrational energy (ZPE) corrections.

3. Results and discussion

3.1. *Structure*

The structure of transition metal dioximato [M(DioxH)$_2$] complexes is square planar (scheme 1) [19]. The complex is established by four donor-acceptor bonds between the metal and the imine nitrogens. In addition to donor-acceptor interactions, an

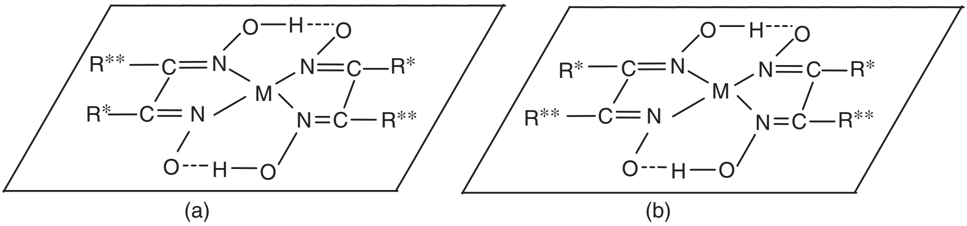

Scheme 1. Structure of transition metal dioximato [M(DioxH)$_2$] complexes.

electrostatic attraction between the partially negatively charged nitrogens and the metal cation also occurs in these complexes. Strong hydrogen bonding between the OH groups and the deprotonated anionic oxygens is important. The $R^* \neq R^{**}$ substituents on the metal-bis(glyoximato) skeleton can be in trans (scheme 1a) or cis (scheme 1b). The two isomers can be unambiguously distinguished by X-ray diffraction in the solid phase and by NMR spectroscopy in solution. In the NMR spectrum of the trans isomer possessing C_i symmetry the equivalent groups give one resonance (e.g. the proton of the O–H $\cdots$ O hydrogen bridge between 17–18 ppm), whereas in the spectrum of the cis isomer each group is represented by two close lying resonances due to the lowered symmetry [24].

Our DFT computations on [Fe(Me-GlyoxH)$_2$(pyridine)$_2$] gave the usual square planar geometry for the Fe(Me-GlyoxH)$_2$ moiety with axial pyridine ligands coordinated to Fe through the nitrogen (figure 1). The pyridine rings prefer an orientation in which the ortho pyridine hydrogens are above the O–H $\cdots$ O hydrogen bonds. This position is favourable for very weak hydrogen bonding interaction with the deprotonated anionic oxygen, characterised by an O $\cdots$ H distance of 2.41 Å. The trans structure was favoured by 1.8 kJ mol^{-1}.

Selected computed geometrical parameters are given in figure 1. The computed Fe–N bond distances (1.94 Å) are indicative of strong donor-acceptor interactions. In agreement with the X-ray structure of [Fe(DH)$_2$(imidazole)$_2$], the two types of Fe–N bonds in the Fe(Me-GlyoxH)$_2$ moiety differ only slighty (by 0.005 Å). The Fe–N$_{py}$ bond is somewhat weaker at 2.05 Å. The computed O $\cdots$ H distances between the two

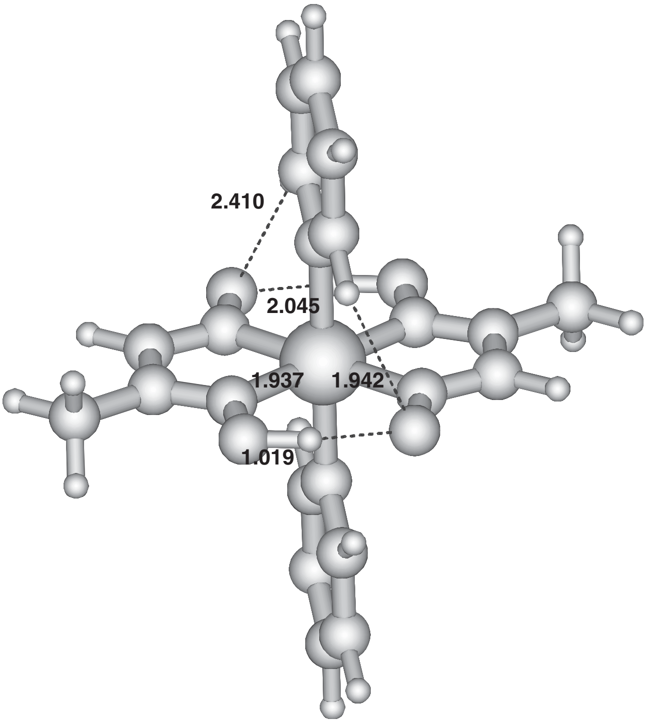

Figure 1. Computed structure of the trans [Fe(Me-GlyoxH)$_2$(pyridine)$_2$] complex and selected computed interatomic distances (Å).

methylglyoximato fragments (1.64 Å) support very strong hydrogen bonding, in agreement with the anionic character of the deprotonated oxygen. Accordingly, the O–H bond is lengthened considerably (to 1.02 Å) upon hydrogen bonding. The geometrical parameters of the trans and cis structures are very similar. The above discussed interatomic distances agree within 0.001 Å in the two structures.

3.2. *FTIR spectra*

The characteristic bands from the FTIR spectra of selected $[Fe(DioxH)_2(amine)_2]$ complexes given in table 2, they are in agreement with the main structural features discussed in the previous section. The assignments of the spectra were based on literature data on various dioximato [25–28] and Fe(II)-pyridine complexes [29]. The assignments presented in table 2 were further supported by our quantum chemical calculations on the $[Fe(Me\text{-}GlyoxH)_2(py)_2]$ complex.

In agreement with the very strong O–H $\cdots$ O hydrogen bond, the OH stretching vibrations ($\nu_{O–H}$) are considerably red-shifted and broadened in the spectra of most

Table 2. Characteristic FTIR data[a] of selected $[Fe(DioxH)_2(amine)_2]$ complexes.

Vibration	$[Fe(DioxH)_2(amine)_2]$						
	3	**6**	**7**	**8**	**10**	**13**	**14**
$\nu_{N–H}$	–	–	3420 m	–	3369 sh	3193 s	3278 s
							3223 s
$\nu_{O–H}$	~2800 br	~2700 br	~2700 br	~2700 br	~2800 br		
$\nu_{C–Har}$	3137 w	3130 s	3095 m	3060 m	3108 s	3062 s	3083 m
	3076 m	3082 sh	3014 s	3026 vs	3021 s	3030 s	3061 m
	3049 s						3041 sh
$\nu_{asC–H}$	2987 w	2977 s	2966 vs	2916 w	2960 m	2920 m	2971 m
	2955 sh	2934 s	2923 s		2923 s		2925 s
$\nu_{sC–H}$	2846 w	2871 s	2833 s	2845 s	2840 w	2850 w	2840 sh
$\delta_{N–O–H} + \nu_{C=N}$	1667 m	1649 m	1640 m	1639 m	1653 m	1675 sh	1627 m
	1520 sh	1528 s	1536 vs	1526 s	1535 vs	1550 s	1550 m
$\nu_{C–Car}$	1620 s	1620 s	1503 m	1601 m	1600 m	1602 s	1604 m
	1509 s	1508 s	1460 s	1493 vs	1493 vs	1494 vs	1495 s
	1460 sh	1478 s		1479 sh	1483 sh	1428 m	1431 vs
δ_{CH_3}	1445 vs	1455 vs	1480 vs	1448 vs	1453 vs	1453 vs	1453 vs
	1383 m	1379 s	1379 s	1375 m	1375 m	1384 vs	1373 m
	1362 sh	1354 s	1354 s	1356 m	1356 vs	1322 s	1328 m
$\nu_{N–O}$	1339 w	1312 m	1308 m	1322 m	1330 s	1321 m	1299 sh
	1242 m	1251s	1247 s	1269 m	1267 m	1205 sh	1197 m
	1213 w	1202 vs	1199 vs	1214 vs	1212 vs	1172 s	1153 w
	1152 s	1136 m	1150 m	1158 sh	1148 m		
$\beta_{C–Har}$	1108 m	1094 vs	1088 vs	1096 m	1096 m	1093 s	1103 m
τ_{OH}	1025 s	1015s	1016 s	1032 s	1046 vs	1044 vs	1032 m
	960 m	966 vs	975 s	964 vs	967 vs	971 vs	982 vs
$\gamma_{C–H}$	734 vs	703 s	702 s	702 vs	702 vs	701 vs	703 vs
$\nu_{Fe–Nox}$	506 s	514 vs	514 vs	506 s	506 s	517 m	524 m
	490 s	498 s	504 vs	482 w	498 sh	453 s	508 sh
	429 m	447 s	447 m	453 m	443 s		446 m
$\delta_{C–N–O}$	360 m	365 s	361 vs	371 s	371 s	398 m	384 w
$\nu_{Fe–Nam}$	296 s	285 s	300 m	313 s	314 m	270 sh	279 m
$\delta_{Nam–Fe–Nam}$	248 s	223 m	255 m	242 m	254 m	245 m	254 m
$\gamma_{N–O}$	172 m	153 m	165 vs	170 m	175 m		

[a] Wavenumbers (cm^{-1}) and intensities of the characteristic absorption bands. The abbreviations br, vs, s, m and w mean broad, very strong, strong, medium and weak, respectively.

of the complexes. Because of overlap with the strong CH stretching bands accurate origin of the broad $\nu_{O\text{–}H}$ bands could not be determined and it was estimated to be around 2700–2800 cm^{-1}. On the other hand, the $\nu_{O\text{–}H}$ bands of complexes **13** and **14** could not be distinguished in our spectra. Such phenomenona have been reported for several extremely strong low-barrier hydrogen bonds [30], among others for Ni(DH)$_2$ [26]. It was explained by the formation of an IR continuum resulting in merging of the OH stretching band into the baseline occurring when proton tunneling motion has a continuous energy level distribution [30]. This continuity of energy level differences occurs for easily polarisable hydrogen bonds upon interactions with the environment (e.g., induced dipole interactions between the hydrogen bonds, mutual interactions via proton dispersion forces, a coupling of the proton tunneling with other vibrations). In the case of our complexes, however, the formation of a broad ν_{OH} band hidden by the strong CH stretching bands cannot be excluded.

Other characteristic spectral features of the strong hydrogen bonds in the title complexes are the NOH in-plane deformation and OH torsional modes appearing between 1500–1800 cm^{-1} and 950–1050 cm^{-1}, respectively, shifted to higher wavenumbers with respect to those of the free ligands [25–32]. Our computations indicate that the N–O–H deformation mode is involved in two intense fundamental bands at around 1650 and 1550 cm^{-1}, strongly mixed with the C=N stretching mode. The OH torsional vibrations give two strong bands in the IR spectra at around 1030 and 970 cm^{-1} (cf. table 2).

The red-shifts of the $\nu_{C=N}$ bands with respect to those of the free dioximes (1620–1650 cm^{-1}) are in agreement with the formation of strong donor-acceptor Fe–N bonds. They consist of two components: (i) the σ-donation involves a shift of the nitrogen lone pairs towards Fe leading to an increase of the strength of the N–O bond; (ii) the other component is the formation of the retrodative π-bonds between Fe and the coordinated dioximes. The π-type d electrons of Fe are transferred to antibonding molecular orbitals of the delocalized π-bond system of the chelate ring, weakening the π-bond of the C=N bond.

The ν_{Fe-Nox} stretching modes appear between 530 and 440 cm^{-1}, and the ν_{Fe-Nam} modes are around 300 cm^{-1} as strong or medium bands, only marginally influenced by the neighbouring groups. The ν_{N-H} bands of the aromatic amines in complexes **13**–**14** are shifted to lower wavenumber, 3300–3100 cm^{-1}, with respect to the free amines (3500–3300 cm^{-1}). This shift may be due to the Fe–N$_{am}$ donor–acceptor interaction, the probable hydrogen bond appearing between the amino hydrogen and the close lying oxime nitrogen and possible intermolecular hydrogen bonding in the crystal.

The $\nu_{N\text{–}O}$ bands of the free dioximes at 920–960 cm^{-1} are shifted considerably in the complexes to 1120–1330 cm^{-1}, the $\nu_{N\text{–}O}$ vibration of the deprotonated oxygen are higher, and $\nu_{N\text{–}OH}$ lower wavenumber bands. The positions of the $\nu_{C=N}$ and ν_{N-O} bands are very sensitive to the nature of the vicinal R*/R** substituents in the dioxime ligand.

The positions of the $\nu_{C\text{–}H}$, δ_{CH3} and $\gamma_{C\text{–}H}$ bands of the coordinated ligands are not affected by complex formation.

3.3. *Mössbauer measurements*

The ^{57}Fe Mössbauer parameters of the complexes are tabulated in table 3. In accordance with earlier data [2, 12, 15] and the FTIR results discussed above, the isomer shift values show that the valence electrons of the Fe(II) ions take part in the delocalized electron system of the coordinating oxime groups. This effect decreases the population of the 3 d orbitals of Fe(II) and increases the charge density at the nucleus resulting in a low isomer shift value. The high quadrupole splitting values indicate high electric field gradients at the nucleus of Fe(II) due to the strongly anisotropic charge distribution and deformed electronic structure around the iron nucleus. This structure can be explained by the effect of four nitrogen atoms in square planar positions. It is an interesting and important finding in the present series of complexes that the obtained Mössbauer parameters are distributed among three groups depending on the applied ligands, as demonstrated in figure 2. Note that [Fe(GlyoxH)$_2$(γ-picoline)$_2$] is outside of the above mentioned three groups having a

Table 3. Room temperature ^{57}Fe Mössbauer parameters (δ: isomer shift, Δ: quadrupole splitting, Γ: linewidth) of the [Fe(DioxH)$_2$(amine)$_2$] complexes. Isomer shifts are given relative to α-iron.

Formula	δ (mm^{-1} s^{-1})	Δ (mm^{-1} s^{-1})	Γ (mm^{-1} s^{-1}
[Fe(GlyoxH)$_2$(imidazole)$_2$]	0.215(4)	1.406(8)	0.327(8)
[Fe(GlyoxH)$_2$(γ-picoline)$_2$]	0.2059(7)	1.775(2)	0.266(6)
[Fe(Me-Et-GlyoxH)$_2$(pyridine)$_2$]	0.231(1)	1.618(2)	0.330(3)
[Fe(Me-Et-GlyoxH)$_2$(γ-picoline)$_2$]	0.222(3)	1.611(6)	0.360(9)
[Fe(Me-Et-GlyoxH)$_2$(imidazole)$_2$]	0.2217(9)	1.420(2)	0.277(2)
[Fe(Me-Et-GlyoxH)$_2$(benzimidazole)$_2$]	0.2648(8)	1.714(2)	0.265(5)
[Fe(Benz-Me-GlyoxH)$_2$(pyridine)$_2$]	0.233(5)	1.586(9)	0.41(1)
[Fe(Benz-Me-GlyoxH)$_2$(γ-picoline)$_2$]	0.234(3)	1.585(7)	0.28(1)
[Fe(Benz-Me-GlyoxH)$_2$(imidazole)$_2$]	0.216(2)	1.441(3)	0.317(5)
[Fe(Benz-Me-GlyoxH)$_2$(benzimidazole)$_2$]	0.263(5)	1.68(1)	0.30(2)
[Fe(Benz-Me-GlyoxH)$_2$(2-Me-imidazole)$_2$]	0.263(2)	1.609(3)	0.365(6)
[Fe(Benz-Me-GlyoxH)$_2$(NH$_3$)$_2$]	0.230(5)	1.53(1)	0.29(2)

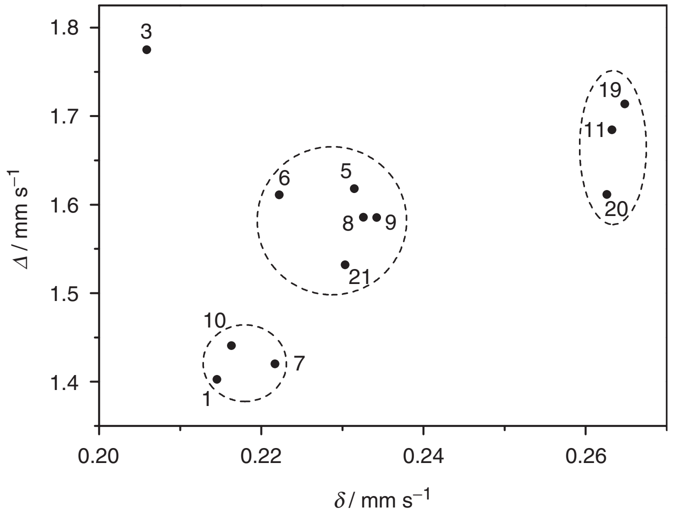

Figure 2. ^{57}Fe Mössbauer isomer shift (δ) and quadrupole splitting (Δ) of the [Fe(DioxH)$_2$(amine)$_2$] complexes measured at room temperature. The numbers around the points correspond to complexes as shown in table 1.

low isomer shift and a high quadrupole splitting parameter. Figure 2 shows clearly that the axial ligands, beside the strong effect of the square planar four nitrogens, have an additional characteristic effect on the electronic structure of Fe(II). The data of figure 2 reveal that increasing isomer shift (δ) increases the quadrupole splitting (Δ). The increasing isomer shift values are a sign of increasing population of the 3d orbitals of Fe(II). This change in electronic structure can lead to an increase of the electric field gradient at Fe(II).

3.4. *Thermal behaviour of the [Fe(DioxH)$_2$(amine)$_2$] complexes*

The Fe(II) complexes decompose upon heating. A dark resinous mass is formed accompanied by evolution of gaseous products. The thermal stability of these mixed dioximine complexes is influenced by the nature of the amine and dioxime ligands and is smaller than those of M(DioxH)$_2$ (M = Ni, Pd). The latter complexes are used for gravimetric analytical purposes. [Fe(DioxH)$_2$(amine)$_2$] complexes possessing low solubility in water were also suggested for gravimetric determination of Fe(II). However, because of unfavourable thermal behaviour, did not enter into analytical practice.

The thermal decomposition data (TG, DTA, DTG) of the [Fe(DioxH)$_2$(amine)$_2$] complexes are presented in table 4. The thermal stabilities of the complexes show the following decreasing trends:

(a) dependence on the dioxime ligand (with the same amine):

$$\mathrm{DH_2 > Me\text{-}Et\text{-}DioxH_2 > GlyoxH_2 > Benz\text{-}Me\text{-}DioxH_2}$$

(b) dependence on the amine ligand (with the same dioxime):
 (i) imidazole > γ-picoline > pyridine > benzimidazole > aromatic amines
 (ii) within the aromatic amines: alkyl-anilines > X-anilines (X = Cl, Br, I)† > naphthylamines

The TG curves show that thermal decomposition begins with the loss of less strongly bonded amine ligands. The two amine molecules leave in one or two steps, as indicated by a slightly expressed inflexion point between 100–150°C on the thermograms. Total deamination takes place in the temperature range of about 150–290°C. Decomposition of Fe(DioxH)$_2$ is a very complicated process showing a slow loss of mass at the conditions of the thermogravimetric measurement. The formation of the Fe(DioxH) intermediary product was not completely stoichiometric up to 450–480°C.

On the basis of the TG data one can presume the following mechanism for thermal decomposition:

$$\mathrm{[Fe(DioxH)_2(amine)_2] \rightarrow [Fe(DioxH)_2(amine)] \rightarrow Fe(DioxH)_2 \rightarrow Fe(DioxH) + DioxH}$$
$$\rightarrow \mathrm{FeO} + \text{various hydrocarbon derivates and dehydration products.}$$

---

†Unpublished results.

Table 4. Thermoanalytical data of selected [Fe(DioxH)$_2$(amine)$_2$] complexes.

			[Fe(DioxH)$_2$(amine)$_2$]									
Method	Step[a]		**1**	**3**	**5**	**8**	**9**	**10**	**11**	**12**	**13**	**14**
TG	–	ΔT (°C)	20–160	20–120	20–165	20–120	20–150	20–40	20–50	20–100	20–60	20–100
	1	ΔT (°C)	160–165	125–132	175–210	120–150	150–170	50–160	50–130	100–218	60–200	100–200
		Calcd (%)	−18.6	−22.4	−15.0	−13.2	−14.9	−11.9	−17.6	−16.4	−18.5	−19.8
		Found (%)	−18.2	−23.0	−14.0[b]	−12[b]	−14[b]	−12.7	−14.5	−18.0[b]	−19–20[b]	−20
	2	ΔT (°C)	165−175	133–145	210–230	150−165	170–185	160–210	140–230	220−290	200–280	200–290
		Calcd (%)	−37.2	−44.7	−30.1	−26.5	−29.6	−23.7	−35	−32.8	−36.8	−39.6
		Found (%)	−38.0	−48	−29.7	−24.0[b]	−30.0	−21.0	−31.5	−32−33[b]	−29.6	−34.6
	3	ΔT (°C)	180–400	150−400	230–235	180–450	190–440	220–450	240−320	300–440	280–440	290–460
		Calcd (%)	−23.8	−20.9	−28.8	−32.1	−30.6	−33.3	−28.4	−29.3	−27.6	−26.4
		Found (%)	−15.2	−21.5	−44.5	−34.0	−29.0	−29	−14	−14.5	−135	−14.5
DTG	1	ΔT (°C)	168	134	191	145	175	38	38	110–130	215	147
	2			141	206	225	221	200	164	217	375–385[c]	180
	3			190–210[c]	225[d]			231	197	420–440[c]		228
									249			360–430[c]
DTA[e]	1	ΔT (°C)	167	144	207	145	172	202	168	80–100	60–70	148
	2	ΔT (°C)	Exo[d]	Endo	Endo	Endo	Endo	Endo	Exo[c]	Exo[c]	Exo	Exo
	3	ΔT (°C)	230–240	153	225	228	176	233	246–348	216	215	180
			Exo[c]	Exo	Exo[d]	Exo	Exo	Exo	Exo	Exo	Exo	Exo
				203	280–400		224					230
				Exo	Exo[c]		Exo					Exo

[a] Step 1: the leave of the first amine ligand; Step 2: the leave of the second amine ligand; Step 3: the leave of 1 mol DioxH ligand.

[b] Inflexion.

[c] Wide, weak.

[d] Very rapid exothermic reaction was observed.

[e] The abbreviations exo and endo mean exothermic and endothermic decomposition processes, respectively.

Table 5. Mass spectral data of selected [Fe(DioxH)$_2$(amine)$_2$] complexes.

Formula	Mol. wt.	m/z (I%)[a]
[Fe(DH)$_2$(pyridine)$_2$]	444	41 (30%)A, 79 (90%)B, 116 (25%)C, 172 (20%)D, 286 (15%)E, 444(80%)M
[Fe(DH)$_2$(imidazole)$_2$]	422	41 (38%)A, 68 (80%)B, 116 (12%)C, 172 (25%)D, 286 (20%)E, 422 (85%)M
[Fe(GlyoxH)$_2$(imidazole)$_2$]	366	41 (35%)A, 68 (70%)B, 88 (20%)C, 143 (31%)D, 230 (33%)E, 69 (24%)F, 366 (70%)M
[Fe(OctoxH)$_2$(γ-picoline)$_2$]	579	41 (25%)A, 93 (80%)B, 169 (20%)C, 224 (18%)D, 393 (25%)E, 579 (25%)M
[Fe(OctoxH)$_2$(imidazole)$_2$]	523	41 (25%)A, 68(40%)B, 169 (10%)C, 224 (45%)D, 393 (38%)E, 530 (100%)M
[Fe(Me-Et-GlyoxH)$_2$(imidazole)$_2$]	452	41 (30%)A, 68(100%)B, 130 (10%)C, 185 (25%)D, 313 (30%)E, 113 (22%)F, 452 (80%)M
[Fe(Benz-Me-GlyoxH)$_2$(pyridine)$_2$]	596	41 (25%)A, 79 (80%)B, 191 (20%)C, 247 (20%)D, 483 (25%)E, 596 (65%)M
[Fe(Benz-Me-GlyoxH)$_2$(imidazole)$_2$]	574	41 (20%)A, 68 (70%)B, 191 (35%)C, 247 (30%)D, 438 (30%)E, 574 (50%)M

[a] Abbreviations of the fragments: A = CH_3CN; B = amine; C = DioxH$_2$; D = Fe(DioxH); E = Fe(DioxH)$_2$; F = furazane; M = molecular ion.

3.5. *Mass spectrometric measurements*

The characteristic mass spectral data of the [Fe(DioxH)$_2$(amine)$_2$] complexes are shown in tables 5 and 6. The appearance of the Fe(DioxH)$_2$, Fe(DioxH), free α-dioxime and amine fragments is in agreement with the above proposed mechanism for the thermal decomposition. Additionally, the peaks of O-heterocyclic furazane fragments appear in the mass spectra, formed by a loss of one H_2O molecule from the dioxime ligands.

The MS data indicate the following decomposition mechanism upon electron impact ionisation at the temperature of the measurement: [Fe(DioxH)$_2$(amine)$_2$] → Fe(DioxH)$_2$(amine)] → [Fe(DioxH)$_2$] → Fe(DioxH) → FeO.

The milder conditions in the electrospray MS measurements facilitated formation of larger adducts from the studied complexes. Peaks of [Fe(DioxH)$_2$(amine)$_2$]DioxH$_2$ and [Fe(DioxH)$_2$(amine)$_2$] furazane adducts appeared in the spectra of the complexes with all the dioxime ligands in the present study (cf. table 6). Hence, formation of the above adducts is not dependent on the type of DioxH$_2$. Intensity of the peaks of DioxH$_2$ and furazane was rather small (1–20%). Formation of adducts seems to be sensitive to the amine ligand. The adducts could not be detected in the spectra of [Fe(Me-Et-GlyoxH)$_2$(imidazole)$_2$] and [Fe(Me-Benz-GlyoxH)$_2$(aniline)$_2$]. Furthermore, [Fe(DioxH)$_2$(amine)$_2$](amine) compounds were not observed in the electrospray MS spectra of the complexes indicating less ability of aromatic and heterocyclic amines to form such adducts.

4. Conclusions

In the present study twenty-one [Fe(DioxH)$_2$(amine)$_2$] complexes have been synthesised and characterised by FTIR, ^{57}Fe Mössbauer, mass spectroscopic and thermal analysis measurements. Quantum chemical computations on [Fe(Me-GlyoxH)$_2$(pyridine)$_2$]

Table 6. Electrospray mass spectral data of selected $[Fe(DioxH)_2(amine)_2]$ complexes.

	m/z (I%)[a]						
Formula	$[FeL_2A_2]$	$[FeL_2A]$	$[FeL_2]$	$[FeL_2A_2]HL$	$[FeL_2A_2]F$	F	HL
$[Fe(GlyoxH)_2(\gamma\text{-picoline})_2]$	416 (30%)	323 (15%)	230 (15%)	503 (11%)	486 (6%)	70 (3%)	(–)
$[Fe(GlyoxH)_2(pyridine)_2]$	389 (30%)	310 (9%)	230 (12%)	476 (1%)	458 (1%)	70 (4.5%)	(–)
$[Fe(Me\text{-}Et\text{-}GlyoxH)_2(\gamma\text{-picoline})_2]$	500 (95%)	407 (12%)	314 (8%)	629 (7%)	611 (1.2%)	112 (6%)	93 (2%)
$[Fe(Me\text{-}Et\text{-}GlyoxH)_2(pyridine)_2]$	472 (–)	393 (13%)	314 (10%)	602 (15%)	584 (3.5%)	112 (8%)	79 (20%)
$[Fe(Me\text{-}Et\text{-}GlyoxH)_2(imidazole)_2]$	450 (88%)	382 (99%)	314 (10%)	580 (–)	562 (–)	112 (22%)	68 (9%)
$[Fe(Benz\text{-}Me\text{-}GlyoxH)_2(\gamma\text{-picoline})_2]$	531 (15%)	531 (15%)	438 (12%)	816 (14%)	799 (7%)	174 (11%)	93 (15%)
$[Fe(Benz\text{-}Me\text{-}GlyoxH)_2(benzimidazole)_2]$	674 (30%)	555 (12%)	438 (13%)	866 (20%)	848 (5%)	174 (12%)	106 (3%)

[a] Abbreviations: L = DioxH ligand; A = amine ligand; F = furazane derivative from the decomposition of $DioxH_2$.

predicted a small (ca $2\,\text{kJ}\,\text{mol}^{-1}$) energy difference between the cis and trans isomers (regarding the relative position of the methyl groups) and very close geometrical parameters in the two structures.

Information on bonding properties was obtained from the FTIR and Mössbauer spectra. The results from both techniques are in agreement with strong Fe–N donor–acceptor interactions. In addition, the characteristic bands of the OH groups support the presence of the very strong (probably low-barrier) hydrogen bonding with the deprotonated anionic dioxime oxygen.

The thermal analysis measurements indicate that thermal decomposition of the complexes goes through the following steps: $[\text{Fe(DioxH)}_2(\text{amine})_2] \rightarrow [\text{Fe(DioxH)}_2(\text{amine})] \rightarrow \text{Fe(DioxH)}_2 \rightarrow \text{Fe(DioxH)} + \text{DioxH} \rightarrow \text{FeO} +$ various hydrocarbon derivates and dehydration products. The fragments observed in the mass spectra suggest the same decomposition upon electron impact ionisation as well.

Acknowledgement

The authors wish to thank Ms. E. Tóth for the thermoanalytical measurements. Fellowships provided for Csaba Várhelyi Jr and Csaba Várhelyi, in every year, by Foundation "Domus Hungarica" to Hungary are gratefully acknowledged. Part of the research was supported by the Hungarian Scientific Research Foundation (OTKA N° T038189). The quantum chemical calculations have been performed on the SUN Fire supercomputer operated by the National Information Infrastructure Development Program of Hungary. A.K. thanks the Bolyai Foundation for support.

References

[1] L.A. Chugaev. *Z. Anorg. Allg. Chem.*, **46**, 144 (1905).
[2] K. Burger, L. Korecz, J.B.A. Manuaba, P. Mag. *J. Inorg. Nucl. Chem.*, **28**, 1675 (1966).
[3] J. Hovák, Z. Finta, Cs. Várhelyi. *J. Inorg. Nucl. Chem.*, **45**, 111 (1981).
[4] F. Feigl. *Spot Tests*, Vol. 1, Elsevier, Amsterdam (1954).
[5] R.C. Fergusson, C.V. Banks. *Anal. Chem.*, **23**, 448 (1951).
[6] C.V. Banks, E.K. Byrd. *Anal. Chim. Acta*, **10**, 129 (1954).
[7] I.M. Peskova, V.M. Savostina, E.K. Ivanova, Oksimi, Izdatelystvo Nauka, Moskova (1977).
[8] B.A. Jillot, R.J.P. Williams. *J. Chem. Soc.*, 462 (1958).
[9] R.W. Dale, R.J. Williams, P.R. Edwards, C.E. Johnson. *Trans. Faraday Soc.*, **64**, 620 (1968).
[10] J. Charalambous, L.J.B. Haines, W.M. Shutie, F.B. Taylor, R.Mc. Guchan, D. Cunningham. *Polyhedron*, **2**, 587 (1983).
[11] J. Zsakó, Cs. Várhelyi, T. Sárvári. *Stud. Univ. Babeş-Bolyai, Chem.*, **34**, 10 (1989).
[12] L. Korecz, A.A. Saghier, Cs. Várhelyi, K. Burger. *Acta Chim. Acad. Sci. Hung.*, **102**, 27 (1979).
[13] A. Desan, H.B. Naik. *J. Inst. Chem.* (India), **62**, 227 (1990).
[14] H.E. Toma, L.A. Marino. *J. Therm. Anal.*, **36**, 7 (1990).
[15] L. Nagy, J. Zsakó, Cs. Novák, Cs. Várhelyi, Gy. Vankó, Gy. Liptay. *J. Therm. Anal. Calorimetry*, **57**, 433 (1999).
[16] K. Bowman, A.P. Gaughan, Z. Dori. *J. Am. Chem. Soc.*, **94**, 727 (1972).
[17] F. Kubel, J. Strahle. *Z. Naturforsch B. Chem. Sci.*, **38**, 258 (1983).
[18] C.K. Prout, T.J. Wiseman. *J. Chem. Soc.*, 497 (1964).
[19] A. Chakravorty. *Coord. Chem. Rev.*, **13**, 1 (1974).
[20] M.J. Frisch, G.W. Trucks, H.B. Schlegel, G.E. Scuseria, M.A. Robb, J.R. Cheeseman, V.G. Zakrzewski, J.A.M. Jr, R.E. Stratmann, J.C. Burant, S. Dapprich, J.M. Millam, A.D. Daniels, K.N. Kudin, M.C. Strain, O. Farkas, J. Tomasi, V. Barone, M. Cossi, R. Cammi, B. Mennucci, C. Pomelli,

C. Adamo, S. Clifford, J. Ochterski, G.A. Petersson, P.Y. Ayala, Q. Cui, K. Morokuma, A.D. Rabuck, K. Raghavachari, J.B. Foresman, J. Cioslowski, J.V. Ortiz, B.B. Stefanov, G. Liu, A. Liashenko, P. Piskorz, I. Komaromi, R. Gomperts, R.L. Martin, D.J. Fox, T. Keith, M.A. Al-Laham, C.Y. Peng, A. Nanayakkara, C. Gonzalez, M. Challacombe, P.M.W. Gill, B. Johnson, W. Chen, M.W. Wong, J.L. Andres, C. Gonzalez, M. Head-Gordon, E.S. Replogle, J.A. Pople. Gaussian 98 (Revision A.9), Gaussian Inc., Pittsburgh PA (1998).
[21] A.D. Becke. *J. Chem. Phys.*, **98**, 5648 (1993).
[22] C. Lee, W. Yang, R.G. Parr. *Phys. Rev.*, **B41**, 785 (1988).
[23] P.J. Hay, W.R. Wadt. *J. Chem. Phys.*, **82**, 270 (1985).
[24] N.I. Marov, A.D. Panfilov, E.K. Ivanova. *Zhurnal Coord. Khim.*, **1**, 1516 (1975).
[25] M. Avram, Gh.D. Mateescu. *Spectroscopia in infrarosu.* Aplicatii in chimia organica, Ed. Tehnica, Bucuresti, 1966.
[26] A. Szabó, A. Kovács. *J. Mol. Struct.*, **651**–**653**, 547 (2003).
[27] J.E. Caton, Jr., C.V. Banks. *Inorg. Chem.*, **6**, 1670 (1967).
[28] B. Orel, M. Penko, D. Hadži. *Spectrochim. Acta*, **36A**, 859 (1980).
[29] K. Nakamoto. *Infrared and Raman Spectra of Inorganic and Coordination Compounds. Part B: Applications in Coordination, Organometallic and Bioinorganic Chemistry*, p. 23, Wiley, New York (1997).
[30] G. Zundel. In *The Hydrogen Bond*, P. Schuster, G. Zundel, C. Sandorfy (Eds), Chapter 15.5, p. 728, North-Holland Publishing Company, Amsterdam (1976).
[31] G. Keresztury, S. Holly. *Spectrochim. Acta*, **33A**, 29 (1977).
[32] A. Szabó, A. Kovács. *J. Mol. Struct.*, **651**–**653**, 615 (2003).